Received: 13 December 2023 | Revised: 8 April 2024 | Accepted: 9 April 2024

DOI: 10.1002/cm.21864

RESEARCH ARTICLE

CYTOSKELETON WILEY

Prediction of the essential intermolecular contacts for side-binding of VASP on F-actin

Fikret Aydin[1] | Harshwardhan H. Katkar[1] | Alisha Morganthaler[2] | Alyssa J. Harker[2] | David R. Kovar[2] | Gregory A. Voth[1]

[1]Department of Chemistry, The James Franck Institute, and Institute for Biophysical Dynamics, University of Chicago, Chicago, Illinois, USA

[2]Department of Biochemistry and Molecular Biology and Department of Molecular Genetics and Cell Biology, University of Chicago, Chicago, Illinois, USA

Correspondence
Gregory A. Voth, Department of Chemistry, The James Franck Institute, and Institute for Biophysical Dynamics, University of Chicago, Chicago, IL 60637, USA.
Email: gavoth@uchicago.edu

Present addresses
Fikret Aydin, Quantum Simulations Group, Materials Science Division, Lawrence Livermore National Laboratory, Livermore, California, USA; and Harshwardhan H. Katkar, Department of Chemical Engineering, Indian Institute of Technology Kanpur, Kanpur, India.

Funding information
National Institute of General Medical Sciences, Grant/Award Number: R01GM063796; National Institutes of Health, Grant/Award Number: R01GM079265; Department of Defense Army Research Office Multidisciplinary University Research Initiative, Grant/Award Number: W911NF1410403; National Science Foundation Graduate Research Fellowship, Grant/Award Numbers: DGE-1144082, DGE-1746045; NIH Molecular and Cellular Biology Training, Grant/Award Number: T32 GM007183; National Science Foundation, Grant/Award Number: ACI-1548562

Abstract

Vasodilator-stimulated phosphoprotein (VASP) family proteins play a crucial role in mediating the actin network architecture in the cytoskeleton. The Ena/VASP homology 2 (EVH2) domain in each of the four identical arms of the tetrameric VASP consists of a loading poly-Pro region, a G-actin-binding domain (GAB), and an F-actin-binding domain (FAB). Together, the poly-Pro, GAB, and FAB domains allow VASP to bind to sides of actin filaments in a bundle, and recruit profilin–G-actin to processively elongate the filaments. The atomic resolution structure of the ternary complex, consisting of the loading poly-Pro region and GAB domain of VASP with profilin–actin, has been solved over a decade ago; however, a detailed structure of the FAB-F-actin complex has not been resolved to date. Experimental insights, based on homology of the FAB domain with the C region of WASP, have been used to hypothesize that the FAB domain binds to the cleft between subdomains 1 and 3 of F-actin. Here, in order to develop our understanding of the VASP–actin complex, we first augment known structural information about the GAB domain binding to actin with the missing FAB domain-actin structure, which we predict using homology modeling and docking simulations. In earlier work, we used mutagenesis and kinetic modeling to study the role of domain-level binding–unbinding kinetics of Ena/VASP on actin filaments in a bundle, specifically on the side of actin filaments. We further look at the nature of the side-binding of the FAB domain of VASP at the atomistic level using our predicted structure, and tabulate effective mutation sites on the FAB domain that would disrupt the VASP–actin complex. We test the binding affinity of Ena with mutated FAB domain using total internal reflection fluorescence microscopy experiments. The binding affinity of VASP is affected significantly for the mutant, providing additional support for our predicted structure.

KEYWORDS
actin, computation, cytoskeleton, Ena/VASP

Fikret Aydin, Harshwardhan H. Katkar and Alisha Morganthaler are contributed equally.

1 | INTRODUCTION

Actin filament network remodeling is important for many cellular processes, such as migration and environment sensing. Among a number of proteins that play a key role in mediating the filament network assembly and growth are the enabled/vasodilator-stimulated phosphoprotein (Ena/VASP) family proteins. Ena/VASP acts as actin filament elongation factor that localizes to regions with diverse networks undergoing dynamic filament remodeling (Krause et al., 2003). Ena/VASP competes with capping protein (Chereau et al., 2005) for barbed ends at the edge of lamellipodia to initiate filopodia and processively elongate filaments to form bundles of the same length during the maturation of filopodia (Applewhite et al., 2007; Barzik et al., 2005; Bear et al., 2000, 2002; Faix & Rottner, 2006; Winkelman et al., 2014). Although significant progress has been made, our understanding of the Ena/VASP mechanism is not complete. Understanding this mechanism requires detailed information about the binding locations of different domains as well as important protein residues that affect the binding affinity of the key proteins.

Ena/VASP proteins include Ena/VASP homology domain 1 (1–113), polyproline region (118–216), Ena/VASP homology domain 2 consisting of G-actin-binding domain (224–238), F-actin-binding domain (260–278), and coiled-coil region (337–373) (Figure 1). Ena/VASP proteins consist of four identical arm, which are linked by a coiled-coil domain. Each arm, in addition to the coiled-coil domain, consists of the conserved Ena/VASP homology 1 and 2 (EVH1 and EVH2) domains along with a central poly-proline-rich domain (Linda J. Ball et al., 2002; L. J. Ball et al., 2000). The EVH1 domain enables Ena/VASP to bind to numerous proteins, such as vinculin, lamellipodin, zyxin, palladin, and formin (Boukhelifa et al., 2004; Brindle et al., 1996; Krause et al., 2004; Reinhard et al., 1995, 1996), while the poly-proline-rich region enables binding to profilin along with the SH3 domains of other proteins (Ahern-Djamali et al., 1998; Ferron et al., 2007; Hansen & Mullins, 2010). The proline-rich region consists of three distinct poly-Pro sites that are conserved, the regulatory, recruiting, and loading poly-Pro sites (Ferron et al., 2007). The EVH2 domain consists of the globular actin-binding (GAB) domain and the filamentous actin-binding (FAB) domain, along with the C-terminal coiled-coil (CC) domain that mediates tetramerization (Bachmann et al., 1999; Ferron et al., 2007; Kuhnel et al., 2004; Walders-Harbeck et al., 2002). The detailed structures of the EVH1 domain alone, the CC domain alone, and the loading poly-Pro and GAB domains complexed with profilin–actin have been determined (Ferron et al., 2007; Kuhnel et al., 2004; Prehoda et al., 1999). The linker between the poly-Pro and GAB domains is believed to be unstructured, and so is the linker between GAB and FAB domains (Ferron et al., 2007). Furthermore, it has been hypothesized that the FAB domain, due to its homology with the C region of WASP, binds in the cleft between subdomains 1 and 3 of the actin subunit at the barbed end of the elongating filament (Ferron et al., 2007). However, these speculations have not been tested due to lack of evidence.

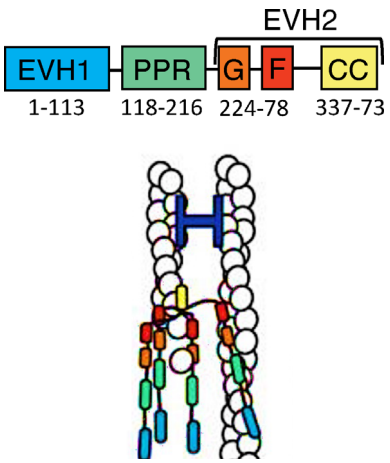

FIGURE 1 Organization of Ena/VASP domains (upper image) and cartoon showing Ena/VASP bound to a trailing barbed end of actin in a fascin bundle (lower image). Ena/VASP domains include: Ena/VASP homology domain 1 (EVH1), polyproline region (PPR), Ena/VASP homology domain 2 (EVH2) consisting of G-actin-binding domain (G), F-actin-binding domain (F), coiled-coil region (CC).

Additionally, our previous work (Harker et al., 2019) highlighted the roles of each of the GAB and FAB domains in efficiently and selectively growing trailing filaments in a bundle. The poly-Pro and GAB domains of Ena/VASP help recruit profilin–actin from the solution and to transfer actin to the barbed end, where it is incorporated into the filament. Meanwhile, the FAB domain plays a crucial role in localizing Ena/VASP by facilitating binding to the sides of actin filaments. Our total internal reflection fluorescence microscopy (TIRFM) experiments with wild-type and mutant Ena suggested that the wild-type tetrameric structure provides an optimum balance between the availability of Ena/VASP arms for recruiting profilin–actin from the solution and the time that Ena/VASP remains bound on a trailing filament end. In particular, we found that side-binding of the FAB domains to neighboring actin filaments in a bundle helps it localize on trailing actin filaments in the bundle. A molecular level understanding of the FAB domain structure and its interactions with actin filaments would therefore enable further progress in deciphering the mechanism of formation of filopodia.

Recent findings on the critical role of Ena/VASP proteins in regulating cytoskeleton network of the cells demonstrate the importance of having a molecular level understanding of Ena/VASP structure and its interactions with actin filaments. Abou-Ghali et al. revealed that Ena/VASP enables polarized actin growth and motility induced by Arp2/3 complex in the absence of capping proteins via collective effects of surface recruitment, bundling activity, and elongation enhancement, and show the importance of different VASP domains on enabling surface polymerization (Abou-Ghali et al., 2020). Other recent work showed that membrane protrusion dynamics can be modulated via interactions of VASP proteins with protein profilin1 (Pfn1), which in turn regulates cell motility (Gau et al., 2019). Furthermore, Damiano-Guercio et al. investigated VASP-dependent changes in the formation of protrusions and their effects on cell migration and adhesion, and found that loss of VASP proteins disrupts lamellipodial architecture and reduces lamellipodial actin assembly (Damiano-Guercio

et al., 2020). They also showed that loss of VASP proteins results in impairment of integrin-mediated adhesion and causes changes in focal adhesion morphologies. In another recent study, Arthur et al. revealed that filopodia initiation in Dictyostelium cells requires VASP protein activity in addition to cortical targeting of MyTH-FERM (MF) Myosin. Their findings demonstrate VASP activities such as actin bundling and polymerization enable MF Myosin activation and this cooperation between the two proteins drives filopodia initiation (Arthur et al., 2021). King et al. investigated the role of Ena/VASP in dorsal vessel (DV) closure and found that loss of Ena impairs DV cell shape and alignment by analyzing DV formation in Ena mutants. They concluded that Ena/VASP enables DV closure by modulating actin cytoskeleton in late cardiac tube formation (King et al., 2021). Visweshwaran et al. showed that dendritic cells rely on three distinct actin nucleation mechanisms to create the actin dynamics that allow efficient migration, while Ena/VASP is a key point of connection between these nucleation pathways (Visweshwaran et al., 2022). Migration of dendritic cells was demonstrated to be substantially hindered in the absence of Ena/VASP proteins. Finally, a recent review provides a comprehensive overview of the current understanding of the molecular mechanisms of Ena/VASP-mediated actin filament assembly, as well as recent findings on the role of Ena/VASP proteins in the cell biological functions related to cell edge protrusion, migration, and adhesion (Faix & Rottner, 2022).

In this work, we use a combination of experiment and atomistic molecular dynamics (MD) simulation in order to study the binding of a single EVH2 domain at the barbed end of an actin filament with the goal of testing certain speculations. Due to the limitations of both the experimental and computational methods for determining binding affinity of proteins, the MD and experiments here are performed in conjunction with one another and the computational methods are used to provide a basis for experimental investigations by predicting effects of mutations on the binding affinity. We use ab initio homology modeling to predict the structure of the linkers that are missing from the detailed structure of loading poly-Pro and GAB domains of human VASP complexed with profilin–actin (PDB entry 2PBD) (Ferron et al., 2007). We further use template-based homology modeling and steered-MD simulations to generate the structure of the FAB domain bound to the actin subunit at the barbed end of the filament. We performed single-point mutation studies in the FAB domain to alter actin–FAB interactions, guided by molecular dynamics simulations, and verified using experiments performed using TIRFM, in order to verify our predicted structure. Our study reveals key residues in the FAB domain that play an important role in modulating side-binding of Ena/VASP, thus providing additional insight into the binding mechanism of this actin-related protein. These findings provide residue-level insight into the functioning of Ena/VASP and augment our earlier domain-level understanding of its actin-binding kinetics. Such detailed insights are essential, for example, for designing drugs targeting predicted critical domains and residues in malfunctioned Ena/VASP.

2 | RESULTS

2.1 | Construction of an initial structure for Ena/VASP interacting with an Actin filament

The development of Artificial Intelligence-derived (AI-driven) structure prediction (i.e., AlphaFold [Jumper et al., 2021] and RoseTTAFold [Baek et al., 2021]) presents a major advance in the ability to generate protein structures quickly. Nonetheless, computational and experimental efforts are still necessary to fully comprehend the underlying mechanisms of a protein's functionality. Proteins exist in both stable, low-energy states and transient, high-energy states. AlphaFold, while capable of predicting a single structure of a protein, does not provide any details regarding the state of the protein. Moreover, there are still some challenges in predicting multi-protein components and binding of small molecules (Moore et al., 2022). To mitigate these issues, various efforts are underway to capture protein interactions, such as AlphaFold Multimer (Evans et al., 2022).

Although the effectiveness of AI approaches in predicting native protein structures is well established, our work focuses on a transient state of proteins, specifically, the transition of an actin monomer from the GAB domain to the barbed end of the elongating filament. Consequently, we constructed our model, particularly the location of FAB domain on the actin filament, based on the mechanism and structure suggested by experimental findings (Ferron et al., 2007).

We built a model of Ena/VASP interacting with an actin filament, by using a crystal structure of Ena/VASP in complex with G-actin (PDB ID: 2PBD) as a starting point for the model (Ferron et al., 2007). The crystal structure is a ternary complex composed of the loading poly-Pro region and G-actin-binding (GAB) domain of Ena/VASP, G-actin, and profilin (Figure 2a). Of the entire EVH2 domain, the PDB structure is missing other poly-Pro regions, the FAB domain, the coiled-coil domain, and two linkers: one connecting the poly-Pro site with the GAB domain and another connecting the GAB domain FAB domain. Of these, we excluded the coiled-coil domain and other poly-Pro regions from this study on the grounds that they presumably do not have any direct interactions with actin (Kuhnel et al., 2004). The fact that linkers are missing in the crystal structure suggests that this region of the protein should not be highly structured. On the other hand, the FAB domain is likely structured and is believed to have a specific binding site on the actin filament. We completed these three parts of the EVH2 domain as follows:

First, the missing linker connecting the loading poly-Pro site and GAB domain was generated by using MODELLER (Eswar et al., 2006; Fiser et al., 2000) based on ab initio homology modeling (Figure 2b). This new complex was placed at the barbed end of an Oda actin filament (Oda et al., 2009) composed of five subunits (actin 5-mer), by superimposing and then substituting the G-actin in the complex with the barbed end actin subunit (labeled A1 in Figure 2c). Our Oda 5-mer actin filament was built as described for a 13-mer filament (Pfaendtner et al., 2010; Saunders & Voth, 2011) by using the actin

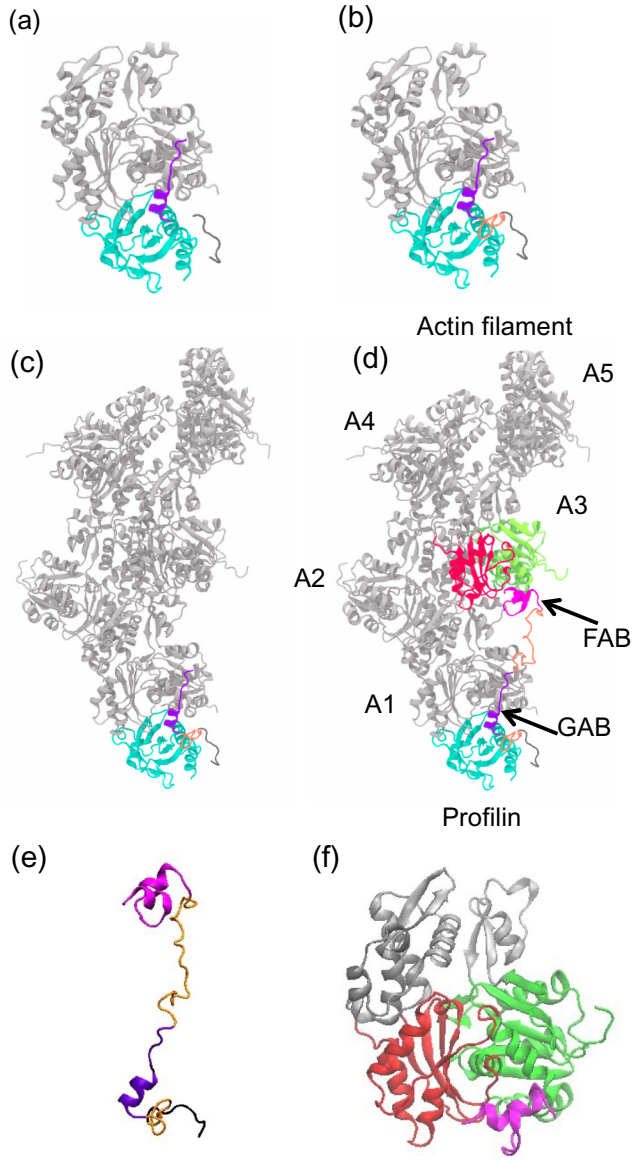

FIGURE 2 Stages of building all-atom structure of Ena/VASP interacting with Oda actin filament. (a) a ternary complex composed of the loading poly-Pro region (black) and G-actin-binding (GAB) domain of Ena/VASP (purple), G-actin (gray) and profilin (cyan). (b) Addition of a linker (orange) connecting GAB and the loading poly-Pro. (c) Alignment of the ternary complex with an actin filament composed of five actin subunits. (d) Modeling of FAB domain (pink) interacting with the cleft between subdomains 1 (red) and 3 (green) of the third actin subunit from the barbed end. (e) Structure of poly-Pro (dark gray), GAB (purple), and FAB (pink) domains and the linkers (orange) between them. (f) Structure of FAB (pink) interacting with the cleft between subdomains 1 (red) and 3 (green) of an actin subunit.

monomer from the Oda structure (PDB:2ZWH) (Oda et al., 2009). The resulting complex captures the state right after the delivery of a profilin–actin to the barbed end by the GAB domain of Ena/VASP (Figure 2c).

We then generated the F-actin-binding (FAB) domain based on template-based homology modeling by using C region of WASP protein as a template (PDB ID: 3P8C—Chain D [Chen et al., 2010] via SWISS-MODEL web server [Arnold et al., 2006; Kiefer et al., 2009]), and connected the FAB domain to the GAB domain via a linker with a length of 21 amino acids (residues 239–259, the sequence is KQEEASGGPTAPKAESGRSGG) (Figure 2d,e). An exact binding site of the FAB domain on the actin filament has not yet been determined, whereas (Ferron et al., 2007) hypothesize that the FAB domain may be interacting with the cleft between subdomain (SD) 1 and SD 3 of the third actin subunit from the barbed end (actin subunit labeled A3 in Figure 2d) based on the known binding site of C region of WASP protein on the actin filament as WASP and Ena/VASP are homologous proteins (Chereau et al., 2005). Based on this hypothesis, we used steered-MD simulations to dock the FAB domain near the actin filament. In order to support the validity of the built complex, we performed protein–protein docking on our FAB-actin monomer (A3) structure using HDOCK server (Yan et al., 2020). Hundreds of models have been generated and scored. Our structure has been assigned to the highest docking score as shown in Table S1.

The barbed end of an elongating actin filament is expected to interact with two different arms of an Ena/VASP protein; therefore, the second subunit from the barbed end is expected to be occupied by another FAB domain. In this proposed mechanism, it is reasonable to assume that the GAB domain bringing an incoming actin monomer to the barbed end is located on the same side with the FAB domain as there is a structural constraint due to a short linker between GAB and FAB domains. Since we model a specific configuration where GAB delivers a new actin subunit to the barbed end, the FAB domain is expected to bind the third subunit due to the structural constraints. On the other hand, the second subunit can be occupied by another FAB domain from a different arm of Ena/VASP protein, which is not included in our simulated structure.

The starting structure of Ena/VASP interacting with F-actin pentamer for all-atom molecular dynamics (AA MD) simulations is shown in Figure 2d. The modeled Ena/VASP structure consists of amino acids from residue 204 to residue 280. After minimization, heating, and equilibrium steps (see Materials and Methods for the details), AA MD simulations were run for 200 ns.

2.2 | Mutations based on predicted structure

The structure predicted by our atomistic simulations consists of the FAB domain placed between subdomains 1 and 3 of the actin subunit A3 in the filament. In order to gain confidence in the predicted structure, we designed single-point mutations in the FAB domain, with the idea that mutations that are based on important contacts between FAB domain and actin in the predicted structure should alter the binding affinity of the FAB domain on actin. To obtain key contacts between the two, we generated another 200-ns-long AA MD simulation trajectory consisting of only the FAB domain of Ena/VASP interacting with a tetrameric actin filament, with the initial structure obtained from our AA MD simulations of the Ena/VASP interacting with the pentameric actin filament. We analyzed the resulting

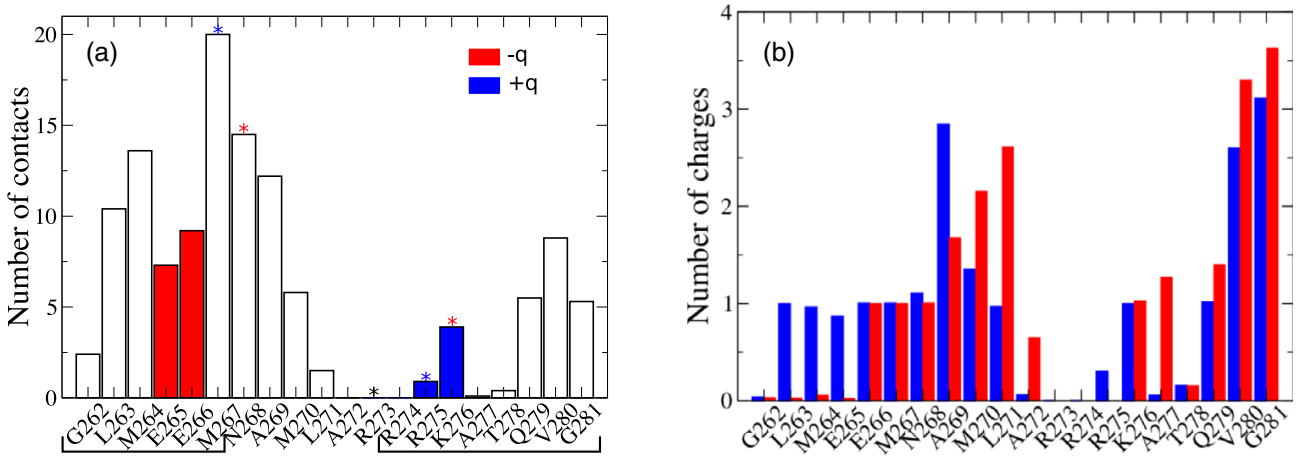

FIGURE 3 Contacts between the FAB domain and actin (a) Number of contacts with actin subunit A3 for each residue in the FAB domain. Brackets on the horizontal axis mark the residues forming the two helices. (b) Number of positively (blue) and negatively (red) charged residues of actin in contact with each residue in the FAB domain.

TABLE 1 Effect of the mutation on stability of the two helices in the FAB domain based on 3.2 ns of MD simulations.

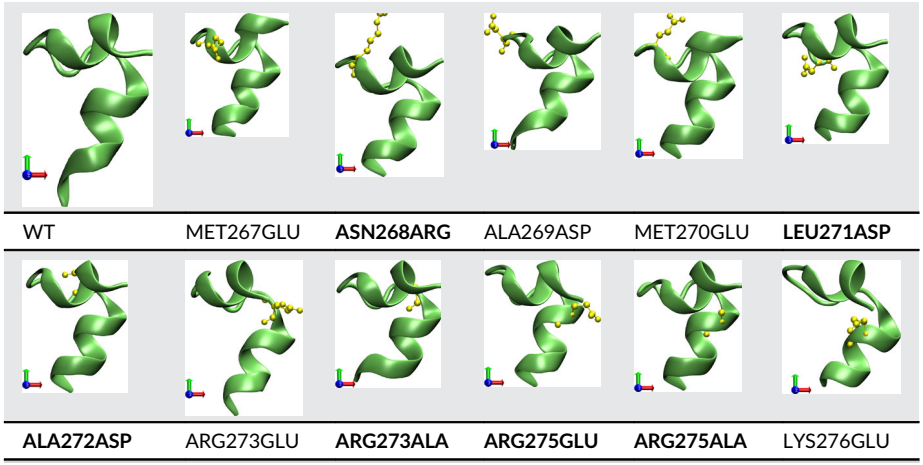

trajectory at the residue level using two approaches. In the first approach, we calculated the average number of contacts (using a 12 Å cutoff distance, average computed over 25 ns) that each residue of the FAB domain makes with the actin subunit A3 in these simulations. The resulting average number of contacts (Figure 3a) clearly shows that the two helically structured regions of the FAB domain have higher number of contacts than the unstructured region between them.

In the second approach, we calculated the average number of positively and negatively charged residues on actin filaments (assuming physiological pH) that are in contact with each residue of the FAB domain. The resulting plot (Figure 3b) shows several key residues of the FAB domain that are surrounded by a large number of charges on the actin residues. We used these results to choose FAB residues for mutation, as described in the following section.

Given the large number of charges on actin that surround several residues of the FAB domain, we chose a number of residues in the FAB domain (listed in Table 1) based on specific properties of the residues (charge, polarity, hydrophobicity), and we then mutated them to a residue that would result in a change in electrostatic interactions between the FAB domain and actin, using the Mutator plugin in VMD (Humphrey et al., 1996). For each of these mutants, we conducted a primary check for the stability of the overall FAB domain structure. We ran a short 3.2 ns AA MD simulation of the mutant FAB domain in water, in order to check the effect of the mutation on stability of the two helices in the FAB domain. If a mutation did not result in disruption of the helices within 3.2 ns of MD simulations (ribbon structure (Frishman & Argos, 1995) corresponding to last frame is shown in Table 1), we continued with further analyzing the mutant. We found that 3.2 ns is long enough to determine whether the mutation results in stable helices, as some mutations cause an immediate disruption of the protein structure due to variation in the ability of amino acids to form protein secondary structures. Of the 11 mutants we considered, six passed this primary check (visually stable helices, marked with a bold font in Table 1) and were selected for subsequent analysis, comprised of AA MD simulations of the mutant FAB domain interacting with an actin filament.

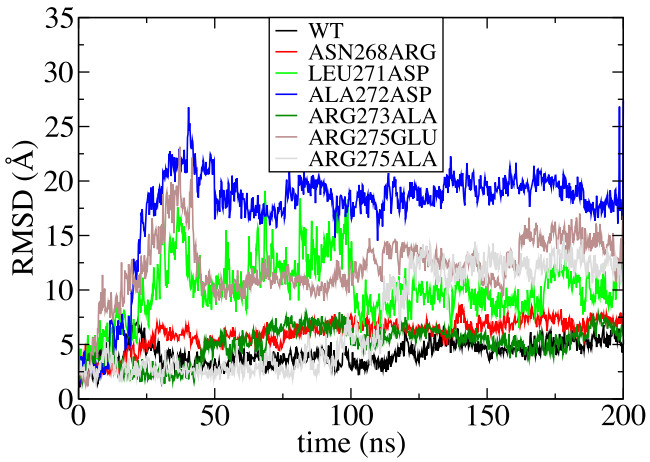

FIGURE 4 Root mean square displacement as a function of time for the wild-type (WT) and mutant FAB domains interacting with an actin filament.

In order to test the effect of each of the six mutants on binding of the FAB domain on actin filament, we performed simulations of these mutant FAB domains interacting with four subunit long actin filaments. The initial structure for these simulations was obtained by superimposing and replacing the FAB domain in the wild-type structure predicted by our AA MD simulations with the mutated FAB domain. Thus, the initial structure for these simulations consisted of the mutated FAB domain of VASP interacting with actin subunit A3, similar to the wild type. The initial structure was then subject to minimization, heating, and equilibration as described in the Methods section. Production runs were performed to obtain a 200-ns-long trajectory. After superimposing the C_α atoms of all residues in the actin filament from each frame with the initial structure at 0 ns as the reference, the root mean square displacement (RMSD) of the C_α atoms of the FAB domain was calculated. The RMSD characterizes the deviation, due to the mutation, from the initial structure predicted by our AA MD simulations. The RMSD is an important metric to compare the stability and functionality of protein structures in computational studies (Aydin et al., 2018; Baker et al., 2015; Doss et al., 2012). The resulting RMSD for the wild-type FAB domain and the six mutants is shown in Figure 4.

The wild-type FAB does not deviate significantly from its initial structure within 200 ns, as indicated by a nearly flat RMSD close to about 5 Å. Similarly, the mutants ASN268ARG and ARG273ALA show a minimal deviation from the initial structure. The mutants LEU271ASP, ALA272ASP, and ARG275GLU show a steep increase in the RMSD, which may be an indication of a weaker affinity of the mutant FAB domain at the binding site of the WT FAB domain on actin filament, although rebinding at alternative sites may still be possible at a longer timescale. Figure S1 shows the distance of each helix from F-actin for these mutants. The mutant ARG275ALA shows a delayed and yet significant increase in the RMSD within 200 ns. Among these mutants, we select the mutant ARG275GLU for our in vitro TIRFM experiments with Ena, with the expectation that the corresponding mutation in Ena (ARG371GLU) would result in a weaker binding affinity of the mutant Ena with actin filaments relative to the wild type. Although the effect of mutations on the stability of proteins has been extensively studied by the experiments, there are various difficulties when introducing mutations to protein complexes. For this reason, we selected the potentially most effective mutation, which also shows a quick initial increase in RMSD but shows a minimal effect on the secondary structure of FAB relative to the WT in our simulation, for subsequent TIRFM experiments.

Our TIRFM data are shown in Figure 5. Representative TIRFM images in Figure 5A qualitatively show the different extent to which Ena coats actin filaments. Quantitative analysis of all TIRFM data reveals that the mutant Ena binds about 6.5 times less compared to the wild type (Figure 5B), in agreement with our expectation based on Figure 4. Representative events showing Ena-mediated elongation of the filaments also demonstrate the shorter residence time of mutant Ena on the barbed end. Although fewer binding events with short residence time are obtained with the mutant Ena, we still observe a measurable fraction of events with residence time longer than 3 s (Figure 5D), confirming that the mutant Ena indeed binds with actin filaments. Our TIRFM analysis clearly shows that the mutant Ena has a significantly lower binding affinity toward actin compared to the wild type. This behavior is consistent with our simulations that predict a weaker interaction between the mutated FAB domain and actin filaments, resulting in a weaker affinity of the mutant Ena for actin. In the future, it will be important to investigate the activities of other mutants, like R273A, to further validate our model predictions.

The importance of the side-binding structure in actin filament interactions cannot be overstated, as it plays a crucial role in regulating actin dynamics and influencing the architecture of sub-cellular structures (Pollard, 2016). While various proteins interact with actin filaments, either at the ends or with the filaments, side-binding proteins exhibit diverse functions, including myosin motors, cross-linkers, bundlers, and severing proteins (Crevenna et al., 2015). Understanding the intricacies of these interactions is essential for unraveling the molecular composition and turnover of structures such as stress fibers and filopodia within cells.

In our study, we focused on the Ena/VASP protein and its side-binding FAB domain, utilizing a combination of computational methods and experimental techniques. Our TIRFM data, presented in Figure 5, illustrate the distinct binding characteristics of the wild-type and mutant Ena proteins. Quantitative analysis revealed a significant reduction in binding affinity for the mutant Ena compared to the wild type, corroborating our computational predictions based on simulations (Figure 4). The shorter residence time of the mutant Ena on the barbed end further emphasized the weakened interaction between the mutated FAB domain and actin filaments.

The broader context of actin filament interactions involves a myriad of regulatory proteins, each contributing to specific cellular functions. For instance, Arp2/3 complex, formins, and proteins with tandem WH-2 domains play pivotal roles in initiating actin filament polymerization, each regulated by nucleation-promoting factors in distinct cellular contexts (Paul & Pollard, 2009; Rouiller et al., 2008).

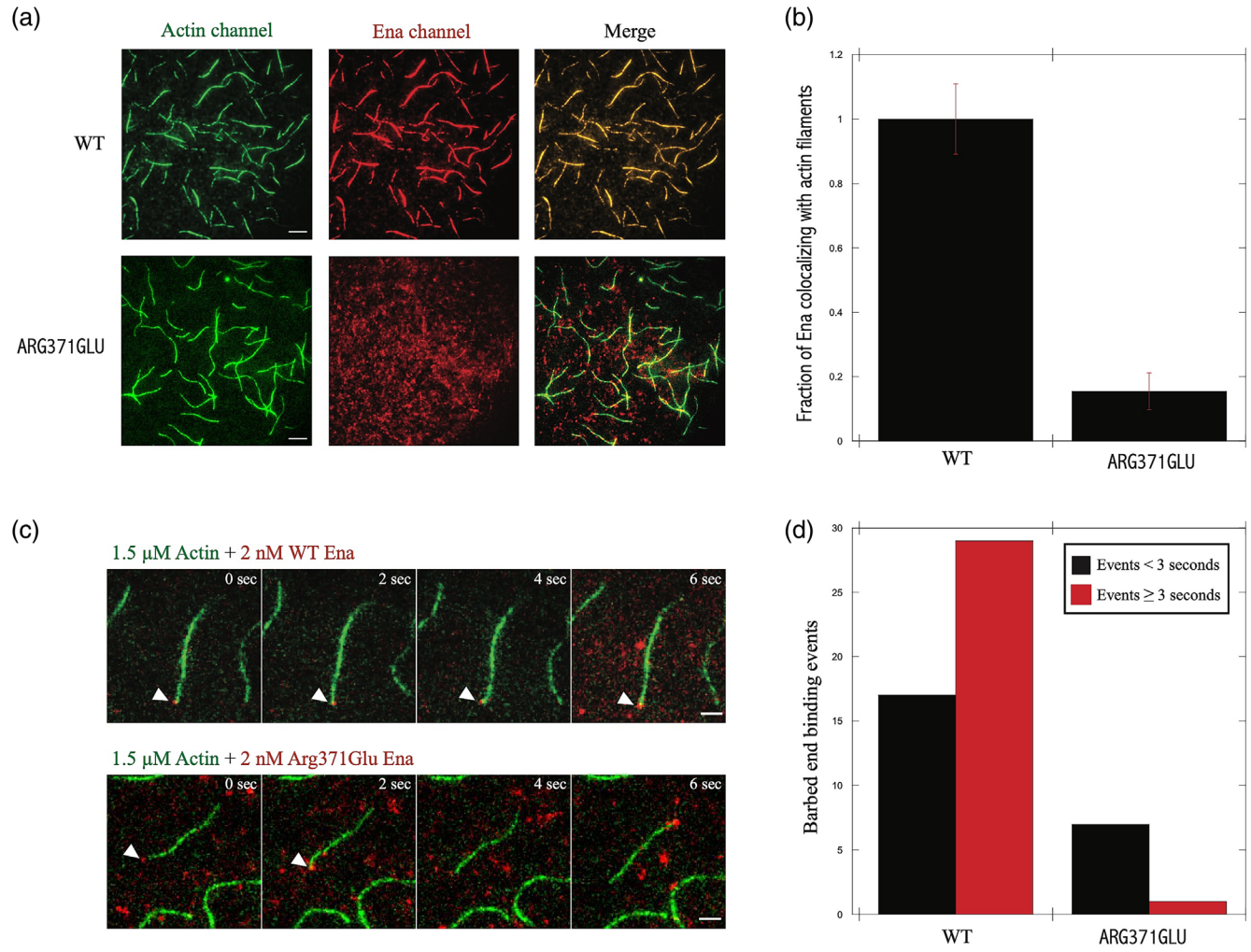

FIGURE 5 Mutation ARG371GLU within the FAB domain of Ena significantly reduces the ability of Ena to bind actin filaments. (a) Representative two color TIRFM images of actin filaments (green) assembled in the presence of WT or mutant Ena (red) (scale bar = 5 μm). The concentration of Ena is 100 nM. (b) Quantification of Ena side-binding along actin filaments. The fraction of Ena colocalizing with actin filament was determined by tracing actin filaments in the 488 channel and measuring the ratio of mean fluorescence of the trace between the 650 Ena channel and 488 actin channel. (c) Ena barbed end elongation events represented by montage images (scale bar = 2 μm). (d) Analysis of barbed end (BE) binding events. When the total length of filaments in the field of view reached ~40 μm, filaments in the field of view were tracked and BE events were quantified until the end of acquisition. WT had significantly more BE events than ARG371GLU and a majority of the witnessed events resided for 3 or more seconds indicating the mutation within the FAB domain is altering the proteins actin filament affinity.

Severing proteins, exemplified by cofilin, contribute to filament dynamics, influencing cellular processes such as motility and cytokinesis (Galkin et al., 2011). Gelsolin family members, acting as filament-severing and capping proteins, showcase the complexity of regulatory mechanisms (Nag et al., 2013). Cross-linking proteins, with their ability to stabilize higher-order structures, and filament-binding proteins like tropomyosin, add another layer of complexity to the intricate network of actin filament interactions (von der Ecken et al., 2015). Understanding the detailed mechanisms of these proteins is critical for unraveling the dynamic regulation of actin filaments in cellular processes.

The FAB domain of Ena/VASP shares similarities with the C region of WASP, suggesting a connection to the WH2 domain (Chereau & Dominguez, 2006). Specifically, the GAB-FAB in Ena/VASP is related to the WH2-C domain in WASP. WH2 domains are frequently found in tandem repeats, which may suggest that GAB-FAB and WH2-C could be viewed as special forms of tandem WH2 domains (Ferron et al., 2007). The GAB-FAB and WH2-C can have different functions in regulating actin filament dynamics (e.g. the GAB-FAB plays role in filament elongation whereas WH2-C is important for Arp2/3 activation). In contrast, other actin-binding proteins may have distinct structural motifs and functions, such as cofilin, which play a role in severing actin filament (Galkin et al., 2011).

In conclusion, this study not only deepens our understanding of the Ena/VASP FAB domain's side-binding structure but also contextualizes it within the broader landscape of actin-binding proteins. The intricate interplay between various actin-binding proteins highlights the complexity of cellular regulation, emphasizing the need for

comprehensive investigations to understanding the molecular details governing these interactions.

3 | CONCLUSIONS

In summary, we have used a combination of ab initio homology modeling, steered-MD, and AA MD simulations in order to complete the partially known structure of the EVH2 domain of Ena/VASP bound to an actin filament. The FAB domain, which is responsible for binding of the Ena/VASP to sides of actin filaments, is placed at its potential binding site in the cleft between subdomains 1 and 3 of F-actin.

AA MD simulations were further used to predict potential single-point mutation in the FAB domain based on the contacts between the FAB domain and F-actin, and TIRFM experiments were used to test the effect of mutation on Ena's binding affinity on actin, confirming the effects predicted from the lead computational predictions. Our work provides significant evidence for the hypothesized FAB domain binding site on an actin filament. More detailed future investigations should include even more comprehensive mutation analysis augmented by structure determination (e.g., cryo-EM if possible) with additional AA MD simulations.

4 | METHODS

4.1 | AA simulations

The protein complex (Ena/VASP interacting with actin 5-mer) was solvated by leaving enough distance in each direction in the simulation box to prevent interactions of the protein with itself through periodic boundary conditions during the MD simulations. All the residues of the protein complex were modeled in their standard states of protonation at a pH value of 7, and the N-termini of the actin subunits were acetylated. 0.18 M KCl was used to neutralize the systems, and then minimization, heating, and equilibrium dynamics were run on the systems by using NAMD (Phillips et al., 2005) with the Charmm27 force field with CMAP corrections (Mackerell Jr. et al., 2004) to prepare them for production runs. More specifically, the systems were first energy minimized by gradually releasing the restraints, and then, the temperature was incrementally increased to 310 K over 200 ps in the heating phase while still restraining the backbone atoms, ADP and the Mg^{2+} ion. Finally, the restraints were gradually reduced from 10 kcal/mol/Å^2 to 0.1 kcal/mol/Å^2 during the equilibration phase spanning 400 ps. The all-atom MD simulation of the Ena/VASP–actin system with unrestrained dynamics was run for 200 ns.

4.2 | Plasmid construction

The Ena mutant was constructed using a QuikChange site directed mutagenesis kit from Agilent (no. 210519) to insert a point mutation at amino acid residue 371 within the FAB domain of MBP-TEV-SNAP-Ena (delta linker). Wild-type Ena was prepared previously (Harker et al., 2019).

4.3 | Protein purification

Both the mutant and wild-type Ena were prepared as previously described (Harker et al., 2019). The Ena constructs were labeled with SNAP-Surface Alexa Fluor 647 (NEB S9136S). Actin was purified from chicken skeletal muscle acetone powder made within the Kovar lab and gel filtered over Sephacryl S300 beads (Sigma no. S300HR). The gel-filtered monomeric actin was polymerized and labeled with Alexa 488 carboxylic acid succinimidyl ester on surface lysine residues (Life technologies A20000).

4.4 | TIRFM

Slides and coverslips (25 × 75 mm Fisher no. 12–544-4 & 24 × 30 mm Fisher no. 12-545-B) underwent a cleaning and etching protocol and were coated with mPEG-silane (Creative PEGWorks no. PLS-2011). Flow chambers were created using double-sided tape. TIRF images were collected every 1 s using a cellTIRF 4Line system (Olympus, Center Valley, PA) fitted to an Olympus IX-71 microscope with through-the-objective TIRF illumination and an iXon EMCCD camera (Andor Technology, Belfast, UK) (Harker et al., 2019). Experiments were performed by mixing Ca-ATP-actin (10% Alexa 488-actin) with magnesium exchange buffer (50 µM $MgCl_2$, 0.2 mM EGTA) and allowing the solution to incubate for 2 min. TIRF polymerization buffer (10 mM imidazole (pH 7.0), 50 mM KCl, 1 mM MgCl2, 1 mM EGTA, 50 mM DTT, 0.2 mM ATP, 50 mM CaCl2, 15 mM glucose, 20 mg/mL catalase, 100 mg/mL glucose oxidase, and 0.5% (400 centipoise) methylcellulose), water, and Ena constructs (either WT or ARG371GLU) were combined and transferred to the actin solution after 2 min had expired. The combined solutions were added to a flow chamber at room temperature for imaging (Zimmermann et al., 2017).

4.5 | Protein binding calculations

Fluorescence intensity was measured by tracing individual Alex 488 actin filaments or filament bundles. Filament density between movies was kept similar. Filament ROIs were made, and the mean fluorescence of the Alexa 488 actin and SNAP 647 Ena was measured using ImageJ. Background fluorescence was subtracted by creating separate ROIs above or below the measured filament. The ratio of mean fluorescence between the SNAP 647 Ena and Alexa 488 actin was determined using the background subtracted values. The average ratios ($n = 3$) were normalized (WT = 1) and plotted.

4.6 | Barbed end binding calculations

The experiments were performed with 1.5 μM 10% Alexa 488 Mg-ATP actin and 2 nM SNAP-Ena 647 (WT or Mut) in order to see individual Ena tetramers in solution. Barbed end binding events were measured by manually tracking all filament barbed ends in the field of view when the filament length of the TIRFM movie reached ~40 μm. Events are defined as SNAP-Ena 647 fluorescent dots that appear to be associated with a filament barbed end. Events were only included if Ena was present at the barbed end for 2 or more frames. Fluorescent dots that did not change position were assumed to be absorbed to the glass and not included. The number of events for WT and Mut was totaled and separated by events residing less than 3 s and events occurring for 3 or more seconds.

AUTHOR CONTRIBUTIONS

D.R.K. and G.A.V. conceived the study. A.M. and A.J.H. designed and performed the experiments. F.A. and H.H.K. designed and performed modeling/simulations. All authors contributed to writing the manuscript. F.A., H.H.K., D.R.K., and G.A.V. participated in revising the manuscript after the review process.

ACKNOWLEDGMENTS

This material is based upon work supported in part by the National Institute of General Medical Sciences (NIGMS) of the National Institutes of Health (NIH), grants R01GM063796 (to G.A.V) R01GM079265 (to D.R.K.), and in part by the Department of Defense Army Research Office Multidisciplinary University Research Initiative (MURI) grant W911NF1410403, National Science Foundation Graduate Research Fellowship grants DGE-1144082 and DGE-1746045 (to A.J.H.), and the NIH Molecular and Cellular Biology Training Grant T32 GM007183 (to A.J.H.). The computations in this work utilized the Extreme Science and Engineering Discovery Environment, which was supported by National Science Foundation grant number ACI-1548562. Additional computational resources were provided by the Research Computing Center (RCC) at The University of Chicago. We thank Dr. Cristian Suarez for his contributions and helpful discussions.

CONFLICT OF INTEREST STATEMENT

The authors declare no conflicts of interest.

DATA AVAILABILITY STATEMENT

The data that support the findings of this study are available from the corresponding author upon reasonable request.

REFERENCES

Abou-Ghali, M., Kusters, R., Korber, S., Manzi, J., Faix, J., Sykes, C., & Plastino, J. (2020). Capping protein is dispensable for polarized Actin network growth and Actin-based motility. *The Journal of Biological Chemistry*, *295*(45), 15366–15375. https://doi.org/10.1074/jbc.RA120.015009

Ahern-Djamali, S. M., Comer, A. R., Bachmann, C., Kastenmeier, A. S., Reddy, S. K., Beckerle, M. C., Walter, U., & Hoffmann, F. M. (1998). Mutations in drosophila enabled and rescue by human vasodilator-stimulated phosphoprotein (VASP) indicate important functional roles for Ena/VASP homology domain 1 (EVH1) and EVH2 domains. *Molecular Biology of the Cell*, *9*(8), 2157–2171. https://doi.org/10.1091/mbc.9.8.2157

Applewhite, D. A., Barzik, M., Kojima, S. I., Svitkina, T. M., Gertler, F. B., & Borisy, G. G. (2007). Ena/VASP proteins have an anti-capping, independent function in filopodia formation. *Molecular Biology of the Cell*, *18*(7), 2579–2591. https://doi.org/10.1091/mbc.E06-11-0990

Arnold, K., Bordoli, L., Kopp, J., & Schwede, T. (2006). The SWISS-MODEL workspace: A web-based environment for protein structure homology modelling. *Bioinformatics*, *22*(2), 195–201. https://doi.org/10.1093/bioinformatics/bti770

Arthur, A. L., Crawford, A., Houdusse, A., & Titus, M. A. (2021). VASP-mediated Actin dynamics activate and recruit a filopodia myosin. *eLife*, *10*, e68082. https://doi.org/10.7554/eLife.68082

Aydin, F., Courtemanche, N., Pollard, T. D., & Voth, G. A. (2018). Gating mechanisms during Actin filament elongation by formins. *eLife*, *7*, e37342. https://doi.org/10.7554/eLife.37342

Bachmann, C., Fischer, L., Walter, U., & Reinhard, M. (1999). The EVH2 domain of the vasodilator-stimulated phosphoprotein mediates tetramerization, F-Actin binding, and Actin bundle formation. *Journal of Biological Chemistry*, *274*(33), 23549–23557. https://doi.org/10.1074/jbc.274.33.23549

Baek, M., DiMaio, F., Anishchenko, I., Dauparas, J., Ovchinnikov, S., Lee, G. R., Wang, J., Cong, Q., Kinch, L. N., Schaeffer, R. D., Millán, C., Park, H., Adams, C., Glassman, C. R., DeGiovanni, A., Pereira, J. H., Rodrigues, A. V., van Dijk, A. A., Ebrecht, A. C., … Baker, D. (2021). Accurate prediction of protein structures and interactions using a three-track neural network. *Science*, *373*(6557), 871–876. https://doi.org/10.1126/science.abj8754

Baker, J. L., Courtemanche, N., Parton, D. L., McCullagh, M., Pollard, T. D., & Voth, G. A. (2015). Electrostatic interactions between the Bni1p Formin FH2 domain and Actin influence Actin filament nucleation. *Structure*, *23*(1), 68–79. https://doi.org/10.1016/j.str.2014.10.014

Ball, L. J., Jarchau, T., Oschkinat, H., & Walter, U. (2002). EVH1 domains: Structure, function and interactions. *FEBS Letters*, *513*(1), 45–52. https://doi.org/10.1016/s0014-5793(01)03291-4

Ball, L. J., Kühne, R., Hoffmann, B., Häfner, A., Schmieder, P., Volkmer-Engert, R., Hof, M., Wahl, M., Schneider-Mergener, J., Walter, U., Oschkinat, H., & Jarchau, T. (2000). Dual epitope recognition by the VASP EVH1 domain modulates polyproline ligand specificity and binding affinity. *EMBO Journal*, *19*(18), 4903–4914. https://doi.org/10.1093/emboj/19.18.4903

Barzik, M., Kotova, T. I., Higgs, H. N., Hazelwood, L., Hanein, D., Gertler, F. B., & Schafer, D. A. (2005). Ena/VASP proteins enhance Actin polymerization in the presence of barbed end capping proteins. *Journal of Biological Chemistry*, *280*(31), 28653–28662. https://doi.org/10.1074/jbc.M503957200

Bear, J. E., Loureiro, J. J., Libova, I., Fassler, R., Wehland, J., & Gertler, F. B. (2000). Negative regulation of fibroblast motility by Ena/VASP proteins. *Cell*, *101*(7), 717–728. https://doi.org/10.1016/s0092-8674(00)80884-3

Bear, J. E., Svitkina, T. M., Krause, M., Schafer, D. A., Loureiro, J. J., Strasser, G. A., Maly, I. V., Chaga, O. Y., Cooper, J. A., Borisy, G. G., & Gertler, F. B. (2002). Antagonism between Ena/VASP proteins and Actin filament capping regulates fibroblast motility. *Cell*, *109*(4), 509–521. https://doi.org/10.1016/s0092-8674(02)00731-6

Boukhelifa, M., Parast, M. M., Bear, J. E., Gertler, F. B., & Otey, C. A. (2004). Palladin is a novel binding partner for Ena/VASP family members. *Cell Motility and the Cytoskeleton*, *58*(1), 17–29. https://doi.org/10.1002/cm.10173

Brindle, N. P. J., Holt, M. R., Davies, J. E., Price, C. J., & Critchley, D. R. (1996). The focal-adhesion vasodilator-stimulated phosphoprotein

(VASP) binds to the proline-rich domain in vinculin. *Biochemical Journal*, *318*, 753–757. https://doi.org/10.1042/bj3180753

Chen, Z., Borek, D., Padrick, S. B., Gomez, T. S., Metlagel, Z., Ismail, A. M., Umetani, J., Billadeau, D. D., Otwinowski, Z., & Rosen, M. K. (2010). Structure and control of the Actin regulatory WAVE complex. *Nature*, *468*(7323), 533–538. https://doi.org/10.1038/nature09623

Chereau, D., & Dominguez, R. (2006). Understanding the role of the G-Actin-binding domain of Ena/VASP in Actin assembly. *Journal of Structural Biology*, *155*(2), 195–201. https://doi.org/10.1016/j.jsb.2006.01.012

Chereau, D., Kerff, F., Graceffa, P., Grabarek, Z., Langsetmo, K., & Dominguez, R. (2005). Actin-bound structures of Wiskott-Aldrich syndrome protein (WASP)-homology domain 2 and the implications for filament assembly. *Proceedings of the National Academy of Sciences of the United States of America*, *102*(46), 16644–16649. https://doi.org/10.1073/pnas.0507021102

Crevenna, A. H., Arciniega, M., Dupont, A., Mizuno, N., Kowalska, K., Lange, O. F., Wedlich-Söldner, R., & Lamb, D. C. (2015). Side-binding proteins modulate Actin filament dynamics. *eLife*, *4*, e04599. https://doi.org/10.7554/eLife.04599

Damiano-Guercio, J., Kurzawa, L., Mueller, J., Dimchev, G., Schaks, M., Nemethova, M., Pokrant, T., Brühmann, S., Linkner, J., Blanchoin, L., Sixt, M., Rottner, K., & Faix, J. (2020). Loss of Ena/VASP interferes with lamellipodium architecture, motility and integrin-dependent adhesion. *eLife*, *9*, e55351. https://doi.org/10.7554/eLife.55351

Doss, C. G., Rajith, B., Garwasis, N., Mathew, P. R., Raju, A. S., Apoorva, K., William, D., Sadhana, N. R., Himani, T., & Dike, I. P. (2012). Screening of mutations affecting protein stability and dynamics of FGFR1-a simulation analysis. *Applied & Translational Genomics*, *1*, 37–43. https://doi.org/10.1016/j.atg.2012.06.002

Eswar, N., Webb, B., Marti-Renom, M. A., Madhusudhan, M. S., Eramian, D., Shen, M. Y., Pieper, U., & Sali, A. (2006). Comparative protein structure modeling using Modeller. *Current Protocols Bioinformatics*, *15*, 5.6.1–5.6.30. https://doi.org/10.1002/0471250953.bi0506s15

Evans, R., O'Neill, M., Pritzel, A., Antropova, N., Senior, A., Green, T., & Hassabis, D. (2022). Protein complex prediction with alphafold-multimer. *bioRxiv*. https://doi.org/10.1101/2021.10.04.463034

Faix, J., & Rottner, K. (2006). The making of filopodia. *Current Opinion in Cell Biology*, *18*(1), 18–25. https://doi.org/10.1016/j.ceb.2005.11.002

Faix, J., & Rottner, K. (2022). Ena/VASP proteins in cell edge protrusion, migration and adhesion. *Journal of Cell Science*, *135*(6), jcs259226. https://doi.org/10.1242/jcs.259226

Ferron, F., Rebowski, G., Lee, S. H., & Dominguez, R. (2007). Structural basis for the recruitment of profilin-Actin complexes during filament elongation by Ena/VASP. *EMBO Journal*, *26*(21), 4597–4606. https://doi.org/10.1038/sj.emboj.7601874

Fiser, A., Do, R. K., & Sali, A. (2000). Modeling of loops in protein structures. *Protein Science*, *9*(9), 1753–1773. https://doi.org/10.1110/ps.9.9.1753

Frishman, D., & Argos, P. (1995). Knowledge-based protein secondary structure assignment. *Proteins*, *23*(4), 566–579. https://doi.org/10.1002/prot.340230412

Galkin, V. E., Orlova, A., Kudryashov, D. S., Solodukhin, A., Reisler, E., Schroder, G. F., & Egelman, E. H. (2011). Remodeling of Actin filaments by ADF/cofilin proteins. *Proceedings of the National Academy of Sciences of the United States of America*, *108*(51), 20568–20572. https://doi.org/10.1073/pnas.1110109108

Gau, D., Veon, W., Shroff, S. G., & Roy, P. (2019). The VASP-profilin1 (Pfn1) interaction is critical for efficient cell migration and is regulated by cell-substrate adhesion in a PKA-dependent manner. *The Journal of Biological Chemistry*, *294*(17), 6972–6985. https://doi.org/10.1074/jbc.RA118.005255

Hansen, S. D., & Mullins, R. D. (2010). VASP is a processive Actin polymerase that requires monomeric Actin for barbed end association. *Journal of Cell Biology*, *191*(3), 571–584. https://doi.org/10.1083/jcb.201003014

Harker, A. J., Katkar, H. H., Bidone, T. C., Aydin, F., Voth, G. A., Applewhite, D. A., & Kovar, D. R. (2019). Ena/VASP processive elongation is modulated by avidity on Actin filaments bundled by the filopodia cross-linker fascin. *Molecular Biology of the Cell*, *30*(7), 851–862. https://doi.org/10.1091/mbc.E18-08-0500

Humphrey, W., Dalke, A., & Schulten, K. (1996). VMD: Visual molecular dynamics. *Journal of Molecular Graphics*, *14*(1), 33-38, 27-38. https://doi.org/10.1016/0263-7855(96)00018-5

Jumper, J., Evans, R., Pritzel, A., Green, T., Figurnov, M., Ronneberger, O., Tunyasuvunakool, K., Bates, R., Žídek, A., Potapenko, A., Bridgland, A., Meyer, C., Kohl, S. A. A., Ballard, A. J., Cowie, A., Romera-Paredes, B., Nikolov, S., Jain, R., Adler, J., … Hassabis, D. (2021). Highly accurate protein structure prediction with AlphaFold. *Nature*, *596*(7873), 583–589. https://doi.org/10.1038/s41586-021-03819-2

Kiefer, F., Arnold, K., Kunzli, M., Bordoli, L., & Schwede, T. (2009). The SWISS-MODEL repository and associated resources. *Nucleic Acids Research*, *37*, D387–D392. https://doi.org/10.1093/nar/gkn750

King, T. R., Kramer, J., Cheng, Y. S., Swope, D., & Kramer, S. G. (2021). Enabled/VASP is required to mediate proper sealing of opposing cardioblasts during drosophila dorsal vessel formation. *Developmental Dynamics*, *250*(8), 1173–1190. https://doi.org/10.1002/dvdy.317

Krause, M., Dent, E. W., Bear, J. E., Loureiro, J. J., & Gertler, F. B. (2003). Ena/VASP proteins: Regulators of the Actin cytoskeleton and cell migration. *Annual Review of Cell and Developmental Biology*, *19*, 541–564. https://doi.org/10.1146/annurev.cellbio.19.050103.103356

Krause, M., Leslie, J. D., Stewart, M., Lafuente, E. M., Valderrama, F., Jagannathan, R., Strasser, G. A., Rubinson, D. A., Liu, H., Way, M., Yaffe, M. B., Boussiotis, V. A., & Gertler, F. B. (2004). Lamellipodin, an Ena/VASP ligand, is implicated in the regulation of lamellipodial dynamics. *Developmental Cell*, *7*(4), 571–583. https://doi.org/10.1016/j.devcel.2004.07.024

Kuhnel, K., Jarchau, T., Wolf, E., Schlichting, I., Walter, U., Wittinghofer, A., & Strelkov, S. V. (2004). The VASP tetramerization domain is a right-handed coiled coil based on a 15-residue repeat. *Proceedings of the National Academy of Sciences of the United States of America*, *101*(49), 17027–17032. https://doi.org/10.1073/pnas.0403069101

Mackerell, A. D., Jr., Feig, M., & Brooks, C. L., 3rd. (2004). Extending the treatment of backbone energetics in protein force fields: Limitations of gas-phase quantum mechanics in reproducing protein conformational distributions in molecular dynamics simulations. *Journal of Computational Chemistry*, *25*(11), 1400–1415. https://doi.org/10.1002/jcc.20065

Moore, P. B., Hendrickson, W. A., Henderson, R., & Brunger, A. T. (2022). The protein-folding problem: Not yet solved. *Science*, *375*(6580), 507. https://doi.org/10.1126/science.abn9422

Nag, S., Larsson, M., Robinson, R. C., & Burtnick, L. D. (2013). Gelsolin: The tail of a molecular gymnast. *Cytoskeleton (Hoboken)*, *70*(7), 360–384. https://doi.org/10.1002/cm.21117

Oda, T., Iwasa, M., Aihara, T., Maeda, Y., & Narita, A. (2009). The nature of the globular to fibrous-Actin transition. *Nature*, *457*(7228), 441–445. https://doi.org/10.1038/nature07685

Paul, A. S., & Pollard, T. D. (2009). Review of the mechanism of processive Actin filament elongation by formins. *Cell Motility and the Cytoskeleton*, *66*(8), 606–617. https://doi.org/10.1002/cm.20379

Pfaendtner, J., De La Cruz, E. M., & Voth, G. A. (2010). Actin filament remodeling by Actin depolymerization factor/cofilin. *Proceedings of the National Academy of Sciences of the United States of America*, *107*(16), 7299–7304. https://doi.org/10.1073/pnas.0911675107

Phillips, J. C., Braun, R., Wang, W., Gumbart, J., Tajkhorshid, E., Villa, E., Chipot, C., Skeel, R. D., Kalé, L., & Schulten, K. (2005). Scalable molecular dynamics with NAMD. *Journal of Computational Chemistry*, *26*(16), 1781–1802. https://doi.org/10.1002/jcc.20289

Pollard, T. D. (2016). Actin and Actin-binding proteins. *Cold Spring Harbor Perspectives in Biology*, *8*(8), a018226. https://doi.org/10.1101/cshperspect.a018226

Prehoda, K. E., Lee, D. J., & Lim, W. A. (1999). Structure of the enabled VASP homology 1 domain-peptide complex: A key component in the spatial control of Actin assembly. *Cell*, *97*(4), 471–480. https://doi.org/10.1016/s0092-8674(00)80757-6

Reinhard, M., Jouvenal, K., Tripier, D., & Walter, U. (1995). Identification, purification, and characterization of a zyxin-related protein that binds the focal adhesion and microfilament protein VASP (vasodilator-stimulated phosphoprotein). *Proceedings of the National Academy of Sciences of the United States of America*, *92*(17), 7956–7960. https://doi.org/10.1073/pnas.92.17.7956

Reinhard, M., Rudiger, M., Jockusch, B. M., & Walter, U. (1996). VASP interaction with vinculin: A recurring theme of interactions with proline-rich motifs. *FEBS Letters*, *399*(1–2), 103–107. https://doi.org/10.1016/s0014-5793(96)01295-1

Rouiller, I., Xu, X. P., Amann, K. J., Egile, C., Nickell, S., Nicastro, D., Li, R., Pollard, T. D., Volkmann, N., & Hanein, D. (2008). The structural basis of Actin filament branching by the Arp2/3 complex. *The Journal of Cell Biology*, *180*(5), 887–895. https://doi.org/10.1083/jcb.200709092

Saunders, M. G., & Voth, G. A. (2011). Water molecules in the nucleotide binding cleft of Actin: Effects on subunit conformation and implications for ATP hydrolysis. *Journal of Molecular Biology*, *413*(1), 279–291. https://doi.org/10.1016/j.jmb.2011.07.068

Visweshwaran, S. P., Nayab, H., Hoffmann, L., Gil, M., Liu, F., Kuhne, R., & Maritzen, T. (2022). Ena/VASP proteins at the crossroads of Actin nucleation pathways in dendritic cell migration. *Frontiers in Cell and Development Biology*, *10*, 1008898. https://doi.org/10.3389/fcell.2022.1008898

von der Ecken, J., Muller, M., Lehman, W., Manstein, D. J., Penczek, P. A., & Raunser, S. (2015). Structure of the F-Actin-tropomyosin complex. *Nature*, *519*(7541), 114–117. https://doi.org/10.1038/nature14033

Walders-Harbeck, B., Khaitlina, S. Y., Hinssen, H., Jockusch, B. M., & Illenberger, S. (2002). The vasodilator-stimulated phosphoprotein promotes Actin polymerisation through direct binding to monomeric Actin. *FEBS Letters*, *529*(2–3), 275–280. https://doi.org/10.1016/S0014-5793(02)03356-2

Winkelman, J. D., Bilancia, C. G., Peifer, M., & Kovar, D. R. (2014). Ena/-VASP enabled is a highly processive Actin polymerase tailored to self-assemble parallel-bundled F-Actin networks with Fascin. *Proceedings of the National Academy of Sciences of the United States of America*, *111*(11), 4121–4126. https://doi.org/10.1073/pnas.1322093111

Yan, Y., Tao, H., He, J., & Huang, S. Y. (2020). The HDOCK server for integrated protein-protein docking. *Nature Protocols*, *15*(5), 1829–1852. https://doi.org/10.1038/s41596-020-0312-x

Zimmermann, D., Homa, K. E., Hocky, G. M., Pollard, L. W., de la Cruz, E. M., Voth, G. A., Trybus, K. M., & Kovar, D. R. (2017). Mechano-regulated inhibition of formin facilitates contractile actomyosin ring assembly. *Nature Communications*, *8*(1), 703. https://doi.org/10.1038/s41467-017-00445-3

SUPPORTING INFORMATION

Additional supporting information can be found online in the Supporting Information section at the end of this article.

How to cite this article: Aydin, F., Katkar, H. H., Morganthaler, A., Harker, A. J., Kovar, D. R., & Voth, G. A. (2024). Prediction of the essential intermolecular contacts for side-binding of VASP on F-actin. *Cytoskeleton*, 1–11. https://doi.org/10.1002/cm.21864